# The Effect of Talc on the Crystallization of Isotactic Polypropylene

MASAHIRO NAIKI,[1] YASUHARU FUKUI,[1] TAKENOBU MATSUMURA,[1] TAKAO NOMURA,[2] MASTOSHI MATSUDA[2]

[1] Ube Industries, Ltd., Nishihon-machi, Ube, Yamaguchi 755-8633, Japan

[2] Toyota Motor Corporation, Toyota-cho, Toyota, Aichi 471-8572, Japan

*Received 19 January 2000; accepted 7 June 2000*

**ABSTRACT:** Isotactic polypropylene (iPP) has been crystallized in the presence of talc under the quiescent state and shear flow of injection molding. The resulting morphology has been investigated by means of polarizing microscopy, transmission electron microscopy, and wide angle X-ray diffraction. In the quiescent state, the iPP lamellae grew from the surface of talc and the transcrystalline region was formed at the interface between iPP melt and the talc. The nucleation of iPP was very frequent on the cleavage plane of talc. The X-ray diffraction pattern of the transcrystal showed $a^*$-axis orientation to the crystal growing direction. In injection-molded samples of the talc-filled iPP, the morphology of lamella growing from talc appeared as same as that of the transcrystal. However, the crystalline orientation of injection-molded talc-filled iPP, in which the $b$ axis was oriented to the thickness direction and the $a^*$ and the $c$ axis was oriented to the flow direction, was quite different from that of the transcrystal. This $b$-axis orientation results from the orientation of the plate plane of talc, which induces the nucleation and the crystallization under shear flow. © 2000 John Wiley & Sons, Inc. J Appl Polym Sci 79: 1693–1703, 2001

**Key words:** isotactic polypropylene; talc; transcrystallization; injection molding; crystalline orientation

## INTRODUCTION

Inorganic fillers such as glass fiber, calcium carbonate, talc, and mica added to polymer improves their rigidity, heat resistance, and dimensional stability. Isotactic polypropylene (iPP) filled with particulate has been widely used in many industrial applications because of its wide variety of physical properties, good mechanical property balances, and low cost.[1] Some of the inorganic fillers in iPP composites often affect the crystallization of the iPP matrix. When a filler induces nucleation of iPP, columnar crystals normal to the filler surface are formed at the interface, because a great many heterogeneous nucleations occur at the surface of filler and the lateral crystal growth is restricted.[2–7] The mechanical properties of the composite materials are greatly dependent on the crystalline structure affected by the filler.

Among fillers for iPP, talc has been used in largest quantity in various applications.[1] The mechanical properties and the crystal structures of talc-filled iPP have been considerably studied.[8–16] It was observed that crystallization temperature and heat of fusion of talc-filled iPP were higher

*Correspondence to:* M. Naiki.

Journal of Applied Polymer Science, Vol. 79, 1693–1703 (2001)

than those of talc-free iPP.[8,10] This indicates that talc induces crystallization of iPP. The crystalline structure of iPP formed in the presence of talc was well examined on injection- and compression-molding specimens.[9,12–14] It was shown that the surface of flaky talc particles was parallel to the surface of the molding specimen, and that the *b* axis of the iPP crystal oriented along the direction normal to the surface of the molding specimen. The orientation of talc is determined by the matrix flow between cavity walls. In addition, Nomura et al.[17] showed the *b*-axis orientation in injection-molded iPP/ethylene–propylene rubber/talc blends.

It may be thought that the *b*-axis orientation of talc-filled iPP in injection molding is attributed to the orientation of flaky talc with cleavage of (002) plane and the effect of the talc that induces crystallization. However, the solidification in injection molding is a complicated process of rapid cooling under shear flow. The interaction between talc and iPP and the nucleation on talc are still obscure, in spite of numerous studies about talc-filled iPP.[8–16] Therefore, it is necessary to elucidate the crystal structure and the crystallization of iPP in the presence of talc under quiescent state before we analyze such a complicated system as injection molding.

In the present work, we investigate the crystallization of iPP on talc surface under quiescent state and show the transcrystallization from talc. The crystalline morphology and the crystalline orientation of growth direction of iPP from talc in quiescent state are compared to those of injection-molded talc-filled iPP. The mechanism of the *b*-axis orientation of injection-molded talc-filled iPP will be also considered.

## EXPERIMENTAL

### Materials

The iPP without additives used in this study was supplied by Grand Polymer Co. Ltd.. It has a weight-average molecular weight $M_w = 1.5 \times 10^4$ and molecular weight distribution $M_w/M_n = 6.8$ determined by gel permeation chromatography and isotactic pentad fraction mmmm = 0.985 determined by $^{13}$C-NMR.

Two kinds of talc with different shapes were used. One was a powder talc, MW HS-T, manufactured by Hayashi Kasei Co. Ltd. with average diameter, 2.75 $\mu$m, and the other was a rock of talc supplied by Shiraishi Calcium Co. Ltd. These talc contain a little aluminum and iron, which are components of chlorite as an impurity—powder, Al $< 0.01\%$ and Fe 0.02%; rock, Al 0.45% and Fe 0.43%—determined by inductively coupled plasma atomic emission spectroscopy (Japan Jarrell-Ash, ICAP-575II). However, the purity of the talc is so high that we need not take account of nucleating effects of impurities.

The rock of talc was cut into plates roughly parallel to the cleavage and perpendicular to it, and the surface was polished using sand paper and diamond paste of 0.25 $\mu$m. We hereafter refer to the cleavage plane of talc and the perpendicular plane to the cleavage as *talc cleavage* and *talc side*, respectively.

### Sample Preparation

Isothermal crystallization was carried out in a temperature-controlled silicone oil bath. The iPP was placed on the polished talc in a test tube under nitrogen atmosphere. The samples were melted at 230°C for 10 min and then quickly transferred to an oil bath preset at the crystallization temperatures. Crystallization times were changed from several hours to several days depending on the crystallization temperatures. After completion of crystallization, thin sections about 10 $\mu$m and ultrathin sections about 100 nm were observed by a polarizing microscope and transmission electron microscopy (TEM), respectively.

iPP samples composed of only transcrystalline layer were prepared by the method of Folkes et al.[18] The iPP was sandwiched between polished talc plates by compression molding and was gradually cooled to room temperature. Transcrystal grew from both interfaces between iPP and talc, and the growing fronts met at the center of the film. It was confirmed that there was no spherulite in the transcrystalline films. After removing the talc, the residual film was used for X-ray diffraction.

The iPP/talc blend, containing 20% of talc powder by weight, was extruded by a Ikegai PCM30 twin-screw extruder at the barrel temperature of 210°C, and the extruded strand was cut into pellets. Sheet specimens(119 $\times$ 69 $\times$1 mm) of iPP and talc-filled iPP were injection molded using a Fanuc Model-30A injection-molding machine under the following conditions: melt temperature 190°C, mold temperature 40°C, and injection speed 100 mm/s.

### Polarizing Microscopy

Thin sections of transcrystals crystallized under isothermal conditions were analyzed using a Nikon OPTIPHOT2-POL polarizing microscope. Isothermal crystallization of iPP in the presence of talc was observed as follows. Thin sections of talc with about 50 $\mu$m thickness were cut and polished using sandpaper, so that the talc cleavage or the talc side might come to the edge. A small amount of iPP placed on a cover glass was melted together with the thin section of talc and was covered by another cover glass. The sandwich was transferred to the hot stage of Linkam LK-600PM heating and cooling apparatus. After it was retained at 230°C for 10 min under nitrogen flow to ensure complete melting, it was cooled at 100°C/min to the crystallization temperatures, and isothermal crystallization was observed by use of polarizing microscope equipped with a CCD camera and a video tape recorder.

### Wide Angle X-Ray Diffraction

Wide angle X-ray diffraction studies were carried out on the transcrystal films, injection-molded iPP, and talc-filled iPP using a Mac Science DIP220 X-ray diffractometor equipped with imaging plate. The X-ray beam was graphite-monochromatized CuK$\alpha$ radiation (40 kV, 250 A).

### Transmission Electron Microscopy

Ultrathin sections of iPP transcrystal and injection-molded specimens were stained by $RuO_4$ and were examined by a JEOL JEM-200CX transmission electron microscope.

### Scanning Electron Microscopy

The surfaces of the powder talc and polished ones were observed using a Hitachi S-4200 scanning electron microscope (SEM).

## RESULTS

### Surface Morphologies of the Talc

The morphology of the talc surface observed by SEM is shown in Figure 1. The powder talc has a flaky shape with step-like cleavage plane [Fig.1(a)]. The surface of the polished talc is rather nonuniform; there are rough and smooth areas. Since talc is so brittle that the weak domains were removed during polishing, a smooth surface could not be obtained. Talc cleavage is composed of many steps of cleavage [Fig.1(b)]. Though the talc side is smoother than the talc cleavage, rough areas also exist [Fig.1(c)]. The steps or rough areas of the talc are considered more effective for inducing the nucleation of iPP than smooth surfaces.

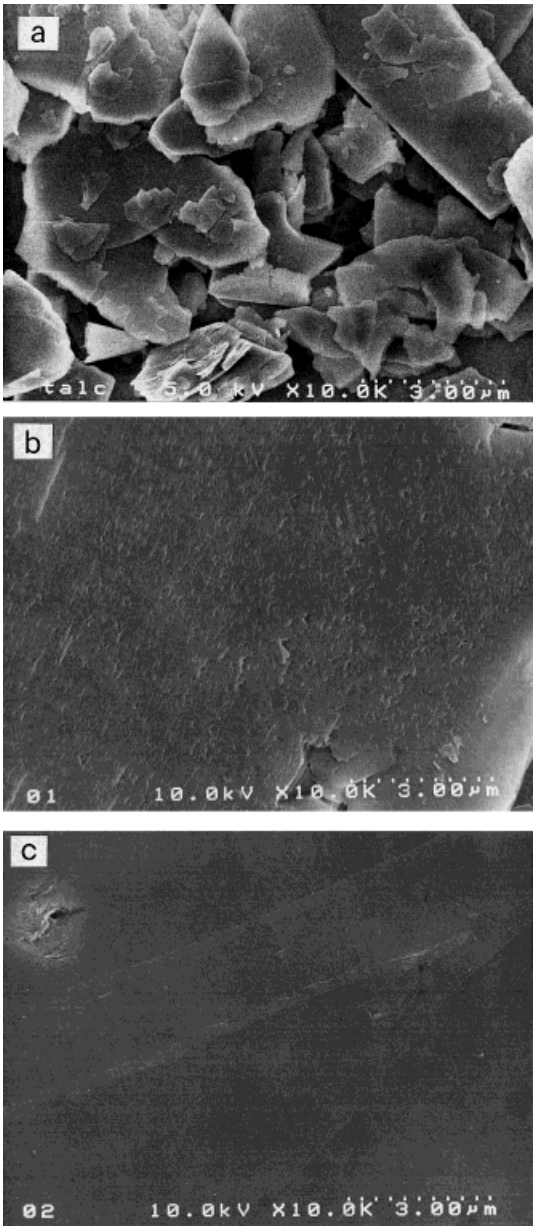


**Figure 1** SEM micrographs of the surface of talc: (a) powder talc, (b) polished talc cleavage, and (c) polished talc side.

### Crystallization Under Quiescent State

Crystallization of iPP in the presence of talc was observed *in situ* by polarizing microscope. Figure

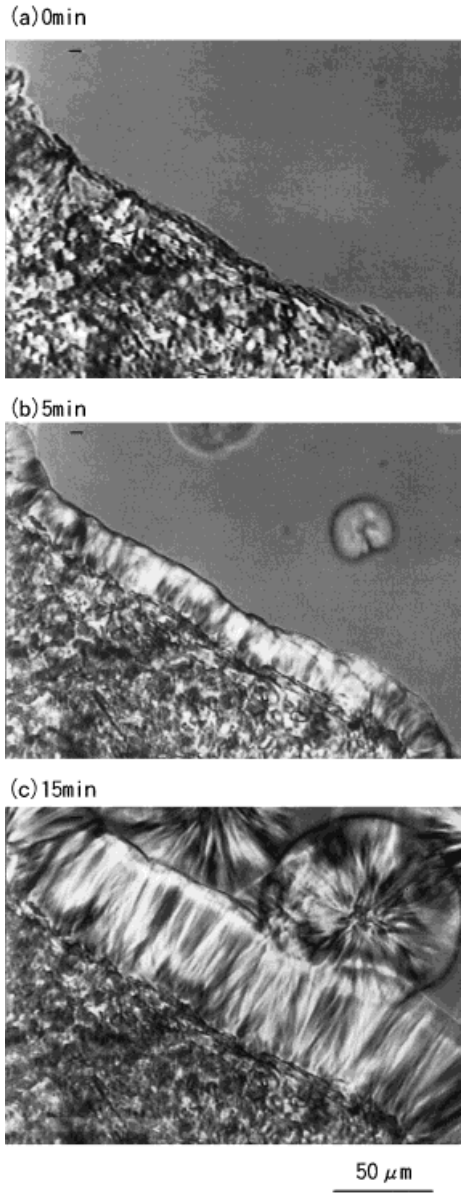


**Figure 2** Polarizing optical micrographs of the crystal growth on the surface of talc at 135°C after 0, 5, and 15 min.

2 shows crystal growth at the iPP/talc interface at 135°C. Molten iPP was in contact with the talc side. Though the crystal was not recognized at the beginning when the temperature just became 135°C, the nucleation at the talc surface and its growth with time was observed. As the surface nucleation density was very large, crystal growth proceeded perpendicular to the talc surface. It was clearly shown that the talc induced crystallization of iPP.

The transcrystal growth continued until it met with a few spherulites that arose in the melt. The growth rate of spherulite and transcrystal is equivalent, since the radius of the spherulite and thickness of the transcrystal are almost equal. Figure 3 shows the transcrystal thickness as a function of time at three different crystallization temperatures. The growth is linear and the growth rate is decreasing with increasing crystallization temperature.

The crystalline morphology of iPP formed from the different planes of talc was analyzed by optical microscope and TEM. Figure 4 shows the optical micrographs of iPP that crystallized isothermally at 135°C from the talc cleavage and the talc side; although the talc existed in the lower part of the photographs, it was removed when the samples were sliced. In both cases, transcrystal region, in which columnar crystals are densely packed, are growing from the interface.

Figure 5 shows the TEM photographs of the interface of the transcrystal crystallized at 150°C on the talc cleavage [Fig. 5(a)] and the talc side [Fig. 5(b)]. In Figure 5(a), the lamellae are arranged perpendicularly to the interface. On the other hand, in Figure 5(b), the lamellae are arranged parallel to the interface. Though, at the level of optical microscopy, the same morphology that the transcrystals grow perpendicular to the talc surface is observed, microscopic observations by TEM show the different arrangement of lamella depending on the talc plane. In either case, the lamella are growing perpendicular to the talc cleavage. Talc is so brittle that, even if we polish the plane normal to the talc cleavage, we may not obtain smooth surface and the step-like talc cleav-

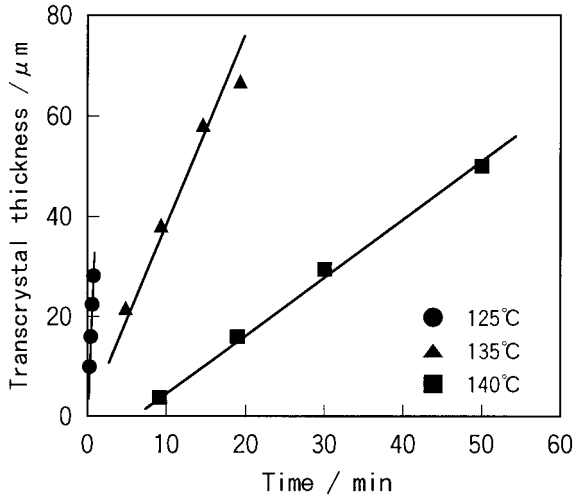


**Figure 3** Growth of the transcrystalline region from talc as a function of time.

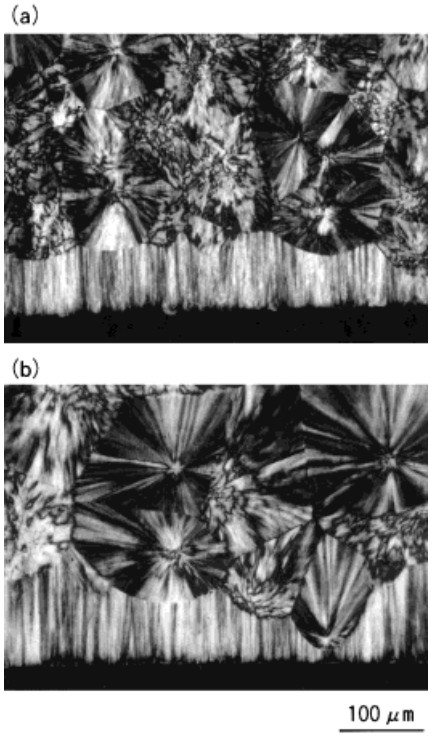


**Figure 4** Polarizing optical micrographs of the transcrystalline region formed from different planes of talc at 135°C: (a) talc cleavage and (b) talc side.

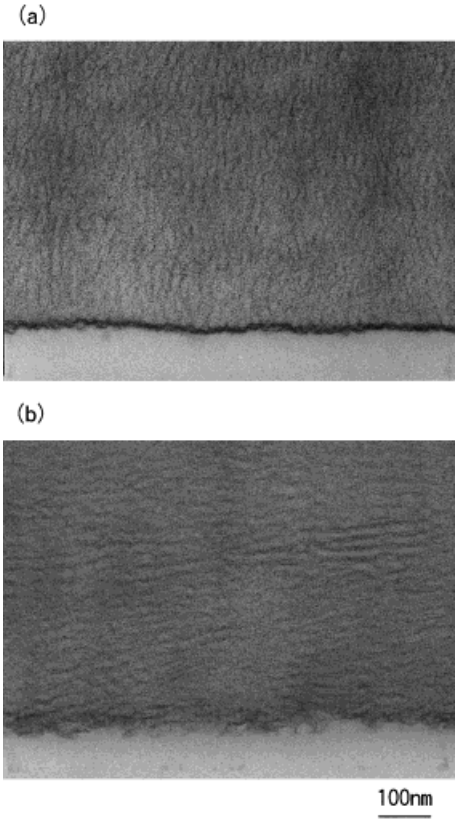


**Figure 5** TEM micrographs of the transcrystal at the interface between iPP and talc. iPP was crystallized on the different planes of talc: (a) talc cleavage and (b) talc side.

age will be exposed. If only a small area of talc cleavage appears, the lamellae can perpendicularly grow there. As a result, the lamellae orient parallel to the interface with talc as shown in Figure 5(b). This is probably because the nucleation on the talc cleavage is more frequent than on the talc side. The lamella in the area at about 10 $\mu$m inside from the interface of the same sample in Figure 5(a) is shown in Figure 6. Besides the dominant lamellae growing from the cleavage plane of talc, there exist a few lamellae perpendicular to the dominant lamellae. This is a characteristic cross-hatched texture of iPP, which is formed homoepitaxially.

### Crystalline Orientation of the Transcrystal

X-ray diffraction patterns of the transcrystals, which grow from the talc sheets, with the talc cleavage and the talc side, are given in Figure 7. The growth direction is horizontal. These patterns show that the crystal are monoclinic ($\alpha$ form). Figure 8 shows the positions of reflections of reciprocal lattice points when rotating the crystal around axes.[19] These were calculated assuming the lattice constant of Natta and Corradini: $a$ = 6.65 Å, $b$ = 20.96 Å, $c$ = 6.5 Å, and $\beta$ = 99.33°.[20] In the edge views of Figure 7, the 110 reflection is clearly observed on the equator and the four 130 arcs in the diagonal direction. Comparison of Fig-

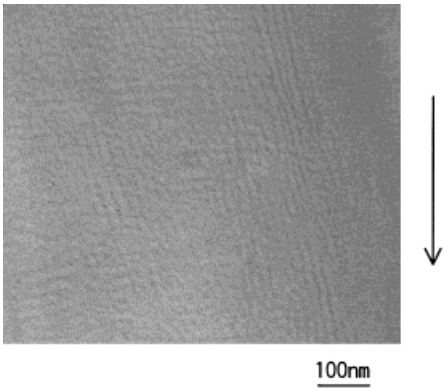


**Figure 6** TEM micrographs of the transcrystal at the inside of 10 $\mu$m from the interface between iPP and talc. The arrow indicates the growth direction of transcrystal.

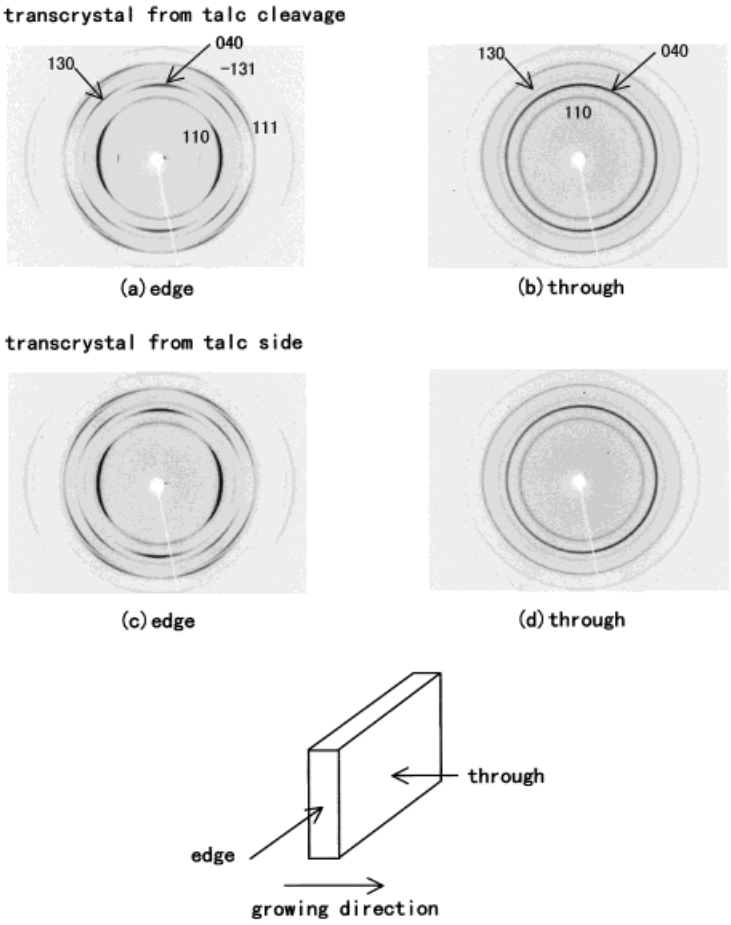


**Figure 7** X-ray diffraction patterns of transcrystal films crystallized from talc cleavage—(a) edge and (b) through—and from talc side: (c) edge and (d) through. The X-ray was transmitted from the through and edge directions as represented in this figure.

ures 7 and 8 shows that the $a^*$ axis is oriented to the growth direction. In addition to the $a^*$-axis orientation, the $c$ axis are slightly oriented to the growth direction, because the 110 reflection is weekly observed on meridian. This $c$-axis orientation results from the homoepitaxial crystalliza-

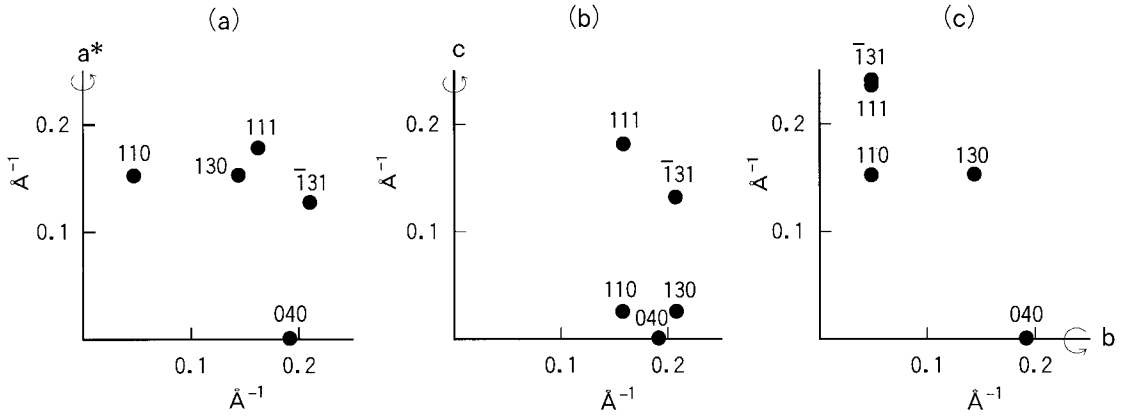


**Figure 8** The positions of reflection of reciprocal lattice points for $a^*$, $c$, and $b$ axis orientation.

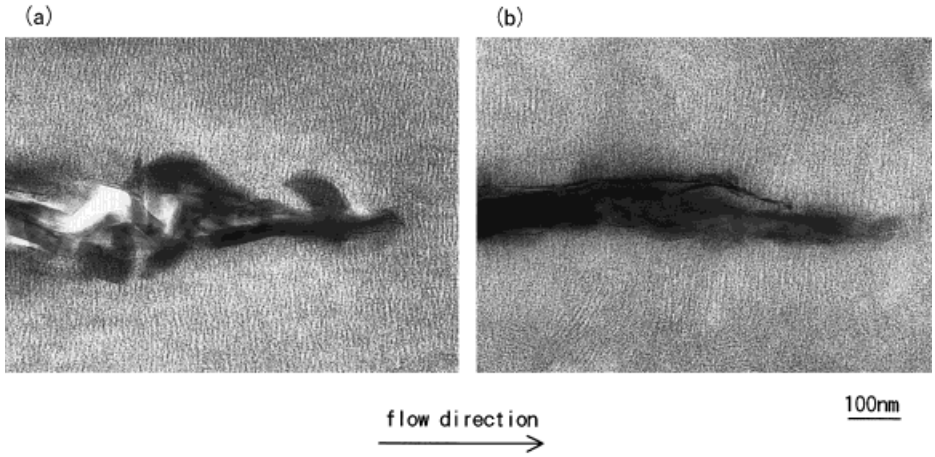


**Figure 9** TEM micrographs of injection-molded talc-filled iPP observed from the edge direction: (a) surface layer and (b) core layer.

tion of the cross-hatched lamellae on the (010) planes of the $a^*$-axis oriented lamellae.[21] On the other hand, the 040 reflection with a ring in the through view shows that the $b$ axis is randomly orientated in the film plane. It can be concluded that the structure of the transcrystal growing from the talc is a cross-hatching texture consisting of the lamellae with the $a^*$ axis parallel to the growing direction and the cross-hatched lamellae that slightly exist. This result agrees well with the TEM observation.

### Crystalline Morphology of Injection-Molded Talc-Filled iPP

Figure 9 shows TEM photographs of the edge view of the injection-molded sheet of talc-filled iPP. The plate-like planes of talc are parallel to the surface of sheet specimen. In the surface layer, the arrangement of the lamellae perpendicular to the talc cleavage is observed. Though, in the core layer, the orientation of lamellae has been slightly disturbed in comparison with the surface layer, it is still preserved.

Figure 10 shows TEM photographs of the edge view of the surface and the core region of the injection-molded sheet of iPP. In the surface layer, the lamellae are arranged perpendicular to the flow direction, which is horizontal in the figures. In the core layer, the lamellae are randomly oriented. This shows the molecular orientation by shear flow relaxed in the core region during solidifying. In comparison with Figures 9 and 10, the

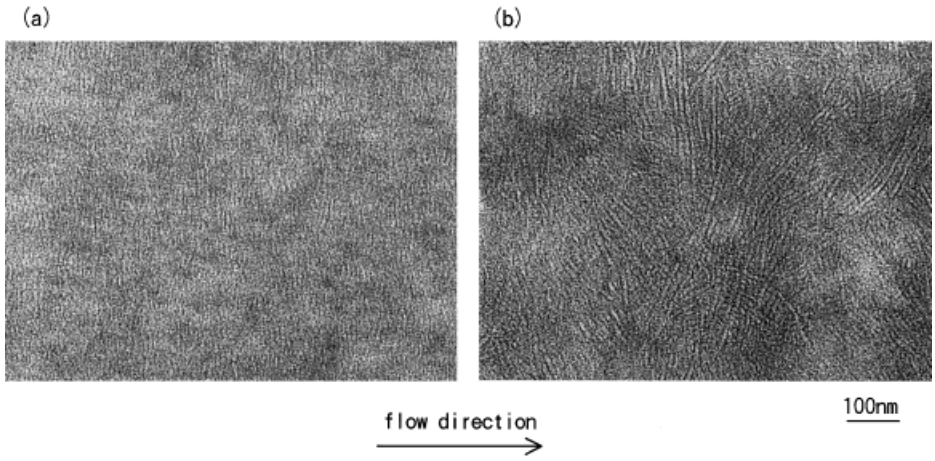


**Figure 10** TEM micrographs of injection-molded iPP observed from edge: (a) surface layer and (b) core layer.

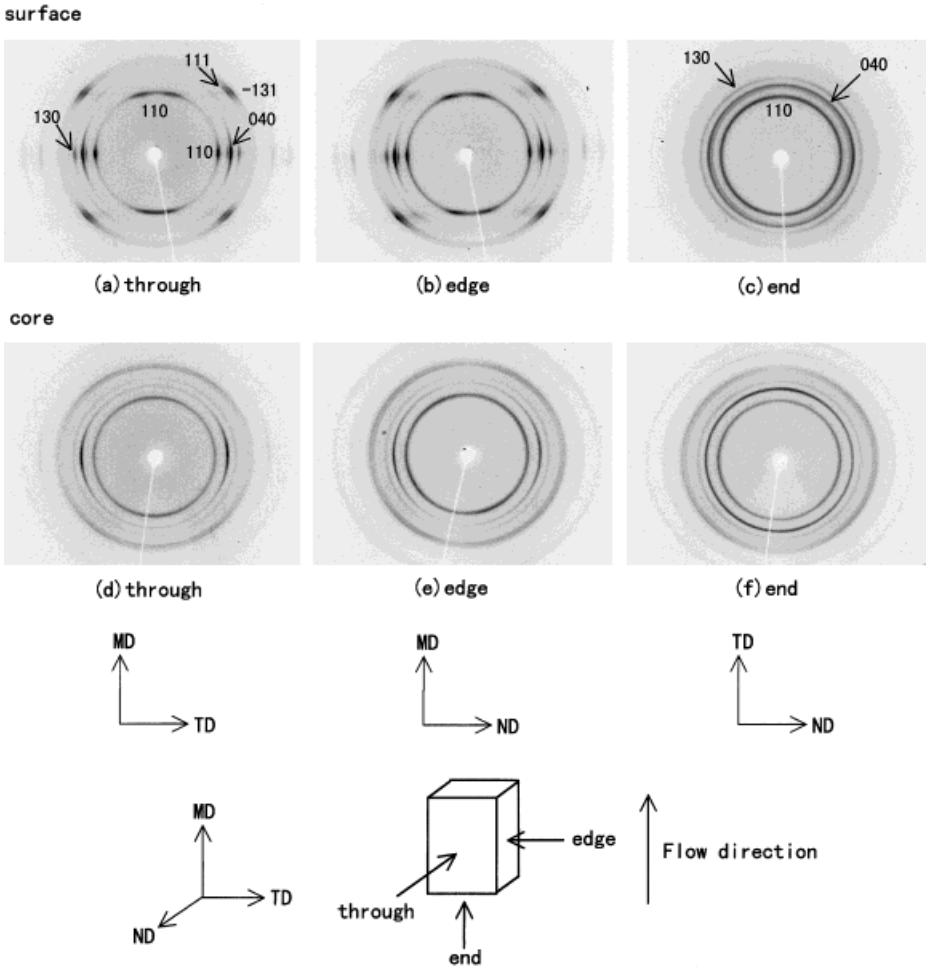


**Figure 11** X-ray diffraction patterns of the surface layer and the core layer of injection-molded iPP: (a)–(c) surface layer, and (d) core layer. X-ray was incident from through, edge, and end directions.

orientation of the lamellae in talc-filled iPP appears more ordered than in iPP. The talc makes the orientation of lamella more ordered.

### Crystalline Orientations of Injection-Molded Talc-Filled iPP

X-ray diffraction patterns of injection-molded iPP and talc-filled iPP are given in Figures 11 and 12, respectively. Figures 11(a)–(c) show those for the surface layer with the thickness of 250 $\mu$m of the injection-molded sheet of iPP taken from the through, edge, and end directions. In both the through and edge views, the 110 reflections are observed on the equator and on the meridian, the 040 reflection on the equator and four points of the 111 and the $-131$ reflections for the meridian. These patterns agree with the *c*- and the $a^*$-axis orientation to machine direction (MD) in reference to Figure 8. The *b* axis is perpendicular to the $a^*$ and *c* axes; the *b* axis is oriented perpendicular to MD. In the end view, the 040 is observed as a ring. Therefore, the *b* axis is randomly oriented around MD. The orientation of the *c* and the $a^*$ axis to the shear flow direction agrees with the literatures.[22, 23] The diffraction at the inside of the 040 on the equator is assigned to the orientated $\beta$ form. Figures 11(d)–(f) are X-ray diffraction patterns of the core layer. In the through and the edge views, there is little orientation of the 110 reflection and the 040 reflection is appreciably concentrated on the equator. The 040 arc is wider than that of the surface layer. In the end view, the 040 reflection is a ring. These results show that the *c* and $a^*$ axes are weakly orientated to the flow direction in the core layer. The crystalline orientation of the core layer is weaker than

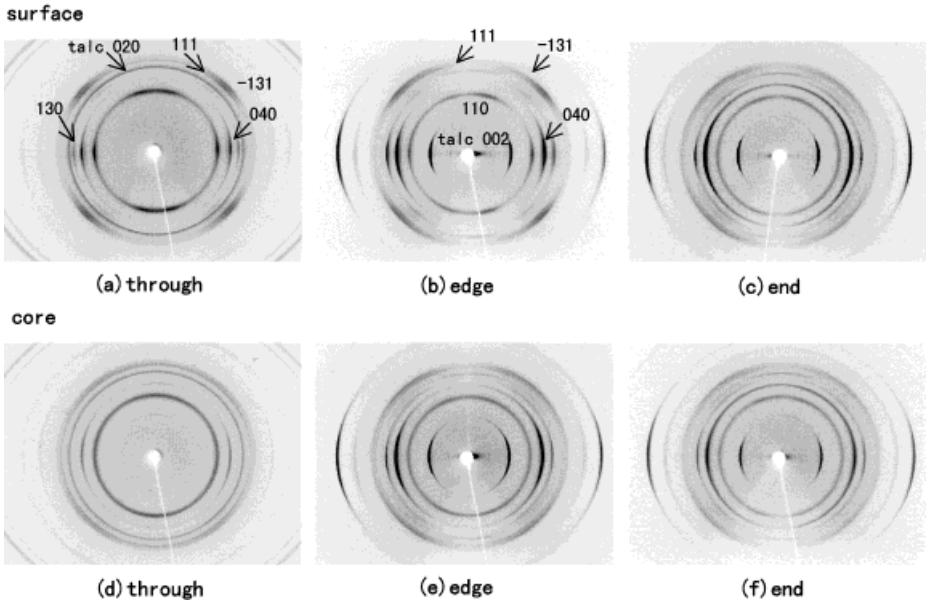


**Figure 12** X-ray diffraction patterns of the surface layer and the core layer of injection-molded talc-filled iPP: (a)–(c) surface layer and (d)–(f) core layer. X-ray was incident from through, edge, and end directions.

that of the surface layer. This agrees with the observations by TEM shown in Figure 9 in which lamellae are more randomly oriented in the core layer.

Figure 12 shows X-ray diffraction patterns for the injection-molded sheet of talc-filled iPP taken from the same directions shown in Figure 11. The diffraction of the talc appears in addition to that of iPP. In the through view, the 020 reflection of talc is observed as a ring. In the edge and the end view, the 020 reflection is not observed and the 002 reflection is on the equator. The talc cleavage is oriented parallel to the surface of the molding sheet. The orientation of talc is also kept in the core layer. The diffraction pattern of iPP in talc-filled iPP resembles that of injection-molded iPP. The orientation of the 110 reflection in the core layer is not so strong as in the surface layer. The *c*- and the *a**-axis orientations to the shear direction are weaker in the core layer than the surface layer. What is different from injection-molded iPP is in the end view where the 040 reflection is observed on the equator. In the edge view, the 040 reflection is observed on the equator. In addition, the 111 and the −131 reflections in the edge view of the surface region are extended to the meridian, which do not show the disorder of the orientation. This is not found in the iPP without talc [Fig. 11(b)]. These indicate that the *b* axis is oriented to the thickness direction of the molded sheet according to Figure 8. Fujiyama et al.[9] and Rybnikář[12] also found the *b*-axis orientation to the thickness direction of injection-molded talc-filled iPP with rectangular or dumbbell shape. Our results agree well with their results.

The above-mentioned results of X-ray studies are summarized as follows: (1) Whether the talc is included or not, the *a** and the *c* axes of iPP are orientated to the flow direction in the surface layer, and the tendency weakens in the inside. (2) When the talc exists, the *b* axis of iPP is orientated to the thickness direction of the sheet. This is completely different from the *a**-axis orientation of the transcrystal from the talc under quiescent state.

## DISCUSSION

We showed the nucleation and its growth of iPP on talc in quiescent state for the first time. When observed by the optical microscopy, the morphology is transcrystal. The growth direction is oriented to the *a**-axis direction, which is the same as that of spherulite.[19, 24] According to the result that the longitudinal direction of the lamella in thin film was parallel to the *a** axis shown by electron diffraction,[24] it is thought that the longer direction of lamella in the transcrystal coincides

with $a^*$ axis. Though the longitudinal direction of the lamella in TEM photographs [Figs. 5(a) and (b)] are different depending on the talc plane that contacts with iPP, the crystal growth direction was along the $a^*$ axis in both cases, as shown by the X-ray diffraction patterns. Hata et al.[25] examined the degree of crystalline orientation of transcrystal of iPP, which grew from polytetrafluoroethylene (PTFE), as a distance from the substrate by microbeam X-ray diffraction. They showed that in the vicinity of PTFE sheet the irregular orientation was observed, and that, at the distance more than 30 $\mu$m, the orientation became more ordered. It seems that the crystalline orientation of the transcrystal growing from talc also become ordered along the $a^*$-axis direction with the distance from the interface.

In injection-molded talc-filled iPP, the crystalline lamella grew from the talc as shown in Figure 9. This reveals that talc has a nucleating ability even under shear flow condition like an injection molding. The $b$ axis of iPP crystal was orientated to the thickness direction. Therefore, the growing direction of the lamella from the talc is oriented to the $b$-axis direction.

Since the crystal orientations of iPP formed from talc are different by crystallization conditions, whether it is under molecular orientation by flow or under static condition, those do not seem to be determined by an epitaxial relationship between a particular crystal plane of iPP and the (002) plane of talc. It can be presumed that talc does not regulate the crystal growth direction but only induces nucleation. This can well explain that, regardless of the existence of the talc, the iPP crystal has the $a^*$-axis orientations in static condition and has $b$-axis orientations perpendicular to the shear flow direction in injection molding.

The $a^*$- and $c$-axis orientation to flow direction, resulting in the $b$-axis orientation perpendicular to the flow direction, are common to injection-molded iPP with and without talc. The difference between them is only the $b$-axis orientation: random orientation around flow direction without talc and orientation to the thickness direction with talc. When talc is included in iPP, the orientation of the $b$ axis is restricted to the thickness direction of the injection-molding sheet. Therefore, in the case of talc-filled iPP, the molecular orientation by shear flow is necessary for the $b$-axis orientation to the thickness direction. In addition, if there is no shear flow, the $a^*$ axis is orientated perpendicular to the talc surface. The

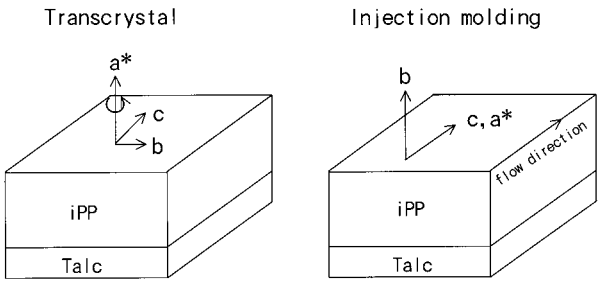


**Figure 13** Schematic representation of crystallographic axis orientations for transcrystal and injection-molded talc-filled iPP.

parallel orientation of plate plane of talc to the surface of the molded sheet must be responsible for the restricted orientation of the $b$ axis to the thickness direction. As the cleavage plane of talc, on which iPP nucleation is very frequent, is oriented parallel to the surface of injection-molded sample, lateral crystal growth and random $b$-axis orientation around the flow direction are inhibited, resulting in $b$-axis orientation to the thickness direction. It is concluded that the $b$-axis orientation injection-molded talc-filled iPP occur as a result of cooperative phenomenon of the nucleation on the oriented talc and the crystallization under shear flow.

The bundles of lamella growing from talc are identical regardless of crystallization conditions under quiescent state or injection molding. But their crystalline orientations along the growing directions are quite different from each other. This situation is schematically described in Figure 13. The crystal growth plane may be different in these cases, but have been little clarified.[26–28] Since the crystal growth is described by the secondary nucleation and growth,[29] the direction of the secondary nucleation seems to be different depending on the crystallization condition whether the molecular orientation by flow or not. Secondary nucleus may arise in the $a^*$-axis direction in transcrystallization and in the $b$-axis direction in injection molding. Under flow condition of injection molding, the molecular chains are orientated to flowing direction. Then the crystallization easily occurs unlike under static condition. The oriented molecules decrease the free energy of the secondary nucleation and are liable to form the secondary nucleus. If we assume that the decrease in the free energy of secondary nucleation is larger in the $b$-axis direction than in the $a^*$-axis direction, the nucleation will occur in the $b$-axis direction and the lamella will grow faster

to this direction than the $a^*$-axis direction. This is thought as one of the reasons why the secondary nucleus are likely to arise in the $b$-axis direction that the intermolecular distance in $b$-axis direction is the smallest. However, further consideration of this problem is necessary, and is a future problem.

## CONCLUSION

Talc induces nucleation of iPP and the transcrystalline region forms at the interface between talc and iPP melt under quiescent condition. The lamella grow perpendicular to the talc cleavage. The nucleation is more abundant on the talc cleavage than on the talc side. The growing direction of the transcrystal is orientated to $a^*$-axis direction.

In the injection-molded talc-filled iPP, the lamella was generated from talc particle. The $a^*$ and $c$ axes are variously oriented to flow direction and the $b$ axis to the thickness direction, which is quite different from that of the transcrystal. The cause of the $b$-axis orientation is ascribed to the orientation of molecular chains by shear flow and the orientation of the plate plane of talc that accelerates the crystallization of iPP.

The authors would like to thank Professor T. Yamamoto of Yamaguchi University, Japan, for helpful discussions.

## REFERENCES

1. Pukánszky, B. Polypropylene Structure, Blends and Composites; Karger-Kocsis, J., Ed.; Chapman & Hall: London, 1995; Vol 3, Chap 1.
2. Misra, A.; Deopura, B. L.; Xavier, S. F.; Hartley, F. D.; Peters, R. H. Angew Makromol Chem 1983, 113, 113–120.
3. Campbell, D.; White, J. R. Angew Makromol Chem 1984, 122, 61–65.
4. Xavier, S. F.; Sharma, Y. N. Angew Makromol Chem 1984, 127, 145–152.
5. Schoolenberg, G. E.; Van Rooyen, A. A. Composite Interfaces 1993, 1, 243–252.
6. Peron, B.; Lowe, A.; Baillie, C. Composites Part A 1996, 27A, 839–845.
7. Thomason, J. L.; Van Rooyen, A. A. J Mater Sci 1992, 27, 889–896.
8. Menczel, J.; Varga, J. J Them Anal 1983, 28, 161–174.
9. Fujiyama, M.; Wakino, T. J Appl Polym Sci 1991, 42, 9–20.
10. Fujiyama, M.; Wakino, T. J Appl Polym Sci 1991, 42, 2739–2747.
11. Rybnikář, F. J Appl Polym Sci 1982, 27, 1479–1486.
12. Rybnikář, F. J Appl Polym Sci 1989, 38, 1479–1490.
13. Suh, C. H.; White, J. L. Polym Eng Sci 1996, 36, 2188–2197.
14. Alonso, M.; Gonzalez, A.; de Saja, J. A.; Requejo, A. Plast Rubber Compos Process Appl 1993, 20, 165–170.
15. Velasco, J. I.; de Saja, J. A.; Martinez, A. B. J Appl Polym Sci 1996, 64, 125–132.
16. Maiti, S. N.; Sharma, K. K. J Mater Sci 1992, 27, 4605–4613.
17. Nomura, T.; Matsuda, M.; Nishio, T.; Hayashi, K.; Wakabayashi, H.; Fujita, Y.; Toki, S. Kobunshi-ronbunsyu 1998, 55, 483–489.
18. Folkes, M. J.; Hardwick, S. T. J Mater Sci Lett 1987, 6, 656–658.
19. Binsbergen, F. L.; De Lange, B. G. M. Polymer 1968, 9, 23–40.
20. Natta, G.; Corradini, P. Nuovo Cimento Suppl 1960, 15, 40–51.
21. Lotz, B.; Wittmann, J. C. J Polym Sci Polym Phys Ed 1986, 24, 1541–1558.
22. Fujiyama, M.; Wakino, T. J Appl Polym Sci 1988, 35, 29–49.
23. Kantz, M. R.; Newman, H. D.; Stigale, F. H. J Appl Polym Sci 1972, 16, 1249–1260.
24. Lovinger, A. J. J Polym Sci Polym Phys Ed 1983, 21, 97–110.
25. Hata, T.; Ohsaka, K.; Yamada, T.; Nakamae, K.; Shibata, N.; Matsumoto, T. J Adhesion 1994, 45, 125–135.
26. Sauer, J. A.; Morrow, D. R.; Richardson, G. C. J Appl Phys 1965, 36, 3017–3021.
27. Kojima, M. J Polym Sci A-2 1967, 5, 597–613.
28. Bartczak, Z.; Galeski, A. Polymer 1990, 31, 2027–2038.
29. Hoffman, J. D.; Miller, R. L. Polymer 1997, 38, 3151–3212.